

www.aem-journal.com

# The Direct Electrospinning and Manipulation of Magic-Sized Cluster Quantum Dots

Haixiang Han, Krista Hirsch, Tobias Hanrath,\* Richard D. Robinson,\* and Larissa M. Shepherd\*

To date, the production of electrospun fibers containing quantum dots (QDs) have required either a carrier material or significant postprocessing. Herein, for the first time, electrospinning only QDs and their ligands using cadmium sulfide (CdS) magic-sized clusters (MSCs) is demonstrated. The key innovation is the exploitation of MSCs synthesized in a stabilizing organic-inorganic mesophase to create fibers consisting of only QDs and their ligands. The atomic structure of the CdS MSCs remains intact throughout the formation of the uniform, continuous, and highly organized ribbon-shaped fibers. For higher applied voltage, thinner fibers with more densely packed structures are achieved as compared with a lower voltage. By electrospinning and manipulating fibers, the hierarchical organization of CdS QDs over six orders of magnitude is highlighted. The onestep, direct fabrication of CdS MSC fibers by traditional electrospinning provides a promising, simple, and economical approach for other types of QDs where continuous high surface area membranes are required. Finally, by embedding fibers into an elastomer matrix, the composite is stretchable (strain,  $\gamma \approx 1.6$ , without breaking), bendable, and able to be braided and woven.

## 1. Introduction

Cadmium sulfide quantum dots (QDs) have unique optical and electronic properties with the potential to be exploited in areas of photovoltaics, catalysis, and chemical sensing. [1–4] For many of these applications, electrospun QD nanofibers have emerged as a convenient and desirable method to form large-area aligned

H. Han, K. Hirsch, R. D. Robinson

Department of Materials Science and Engineering

Cornell University Ithaca, NY 14853, USA E-mail: rdr82@cornell.edu

T. Hanrath

Robert F. Smith School of Chemical & Biomolecular Engineering

Cornell University

Ithaca, NY 14853, USA

E-mail: tobias.hanrath@cornell.edu

L. M. Shepherd

Department of Fiber Science & Apparel Design

Cornell University Ithaca, NY 14853, USA

E-mail: larissa.shepherd@cornell.edu

The ORCID identification number(s) for the author(s) of this article can be found under https://doi.org/10.1002/adem.202100661.

DOI: 10.1002/adem.202100661

electrodes, with high surface area and better charge conduction compared with OD thin films.<sup>[5,6]</sup>

One of the limitations of current QD electrospinning methods, however, is the need for a carrier such as poly(vinyl alcohol) or poly(acrylonitrile) and, often, postprocessing steps.<sup>[7]</sup> In addition, for traditional and colloidal electrospinning, this excess high molecular weight organic matrix generally results in randomly dispersed particles throughout the nanofiber.[7,8] In the case of films, absent a polymer carrier, the mechanical properties of the QD films lack flexibility.<sup>[9]</sup> Nanoribbons produced by chemical vapor deposition (CVD), whereas having a higher surface area than traditional thin films, are not continuous and have a large size distribution (2-40 μm).<sup>[10]</sup> Contrary to films and ribbons, nanowires and fibers generally have better biaxial flexibility, due to

Griffith's criterion which suggests that there is a lower chance of flaws to break a fiber as compared with the bulk material.<sup>[11]</sup> In addition to mechanical flexibility, fibers of QDs also have superior optical and charge transfer performance. <sup>[5,12]</sup> Electrospun fibers, as a special case, have a high surface area, high porosity, are continuous, and generally have a narrower size distribution than nanoribbons produced by CVD. <sup>[10]</sup> These attributes, along with the ability to alter the structural design of electrospun fibers by various methods, <sup>[13]</sup> allows for an intriguing testbed for carrier free, self-assembling CdS magic-sized clusters (MSCs).

While electrospinning without a carrier polymer has proven difficult, it is not impossible. McKee et al. showed that high molecular weight polymers are not essential for electrospinning, but that supramolecular interactions, like lecithin above its critical micelle concentration, can act as chain entanglements for successful electrospinning. [14] Other researchers have more recently used these types of interactions to electrospin small molecule tannic acid. [15] Electrospinning only QDs and their ligands, however, without some type of additional carrier, whether supramolecular, colloidal, or high molecular weight polymer, has not previously been achieved. This challenge of processing derives from QDs having insufficient long-range interparticle interaction for drawing them into continuous fibers.

Recent advances have enabled the synthesis of oleate passivated CdS QDs at high volume fractions and in large quantities as

www.aem-journal.com

"MSCs."<sup>[16]</sup> These MSCs demonstrate unique mesophase behavior that not only stabilizes the ultrasmall nanoclusters, but also provides effective organic–inorganic interactions that foster the formation of an ordered MSC assembly.<sup>[16]</sup> While fibers have been formed from molecules with mesophases, as in wet spun graphene fibers,<sup>[17]</sup> it has yet to be demonstrated that a quantum dot (QD) mesophase, consisting of particle sizes ranging in the few nanometers can be exploited to produce fibers. Therefore, this system provides a compelling opportunity to create a new class of MSC hierarchical materials by direct electrospinning.

In this report, we show how these MSCs can be spun directly into fibers (**Figure 1**). Importantly, the resulting fibers can be manipulated to form macroscopic structures, introducing new prospects for hierarchical systems with programmable structure at multiple length scales. The electrospinning sans polymer is enabled by our observation that MSCs become viscoelastic with a pseudoplastic (shear thinning) behavior when put in suspension (Figure 1A), even at low concentrations (<5 wt% MSC). We then use this MSC dope composed solely of oleic acid (OA) passivated CdS QDs to electrospin fibers through thin nozzles (Figure 1B,C). We report the conditions required for electrospinning these MSC fibers, the fiber's crystal structure, and their incorporation with elastomer to create a pliable testbed for future applications including weaves and braids.

#### 2. Results and Discussion

We produced CdS MSC electrospun fibers with no carrier polymer using a traditional electrospinning apparatus (Figure 1). Briefly, we demonstrated electrospinning fibers using two applied voltages, 7 and 15 kV, at  $\approx$ 14 cm separation from the

target, with a 1.5 mL h<sup>-1</sup> flow rate. Electrospinning CdS MSCs from chloroform resulted in relatively flat, ribbon-shaped fibers with raised edges (Figure 2A,B). Several factors contribute to the ribbon structure observed: 1) the use of only chloroform, a highly volatile solvent, [18] 2) a viscoelastic spinning dope, [19] and 3) relatively high flowrate. [20] Based on these three parameters, the CdS fibers take on the ribbon shape as the result of quick solidification of the fiber sheath thus leading to the collapse of the spherical fiber structure. As expected, at the same distance and flow rate, at higher applied voltage, thinner ribbon widths are produced as a result of the greater stretching experienced at higher voltages. Electrospun fibers produced at 7 and 15 kV have widths of  $2.5 \pm 0.9$  and  $1.3 \pm 0.4 \,\mu\text{m}$ , respectively as measured from field emission-scanning electron microscopy (FE-SEM) images (Figure 2A,B). To better understand the role of the MSC in the fiber spinning process, we carried out a control experiment to electrospin cadmium oleate (Cd(OA)<sub>2</sub>) under the same conditions as we electrospin CdS MSCs. For Cd(OA)2 suspended in chloroform, we could not electrospinning at 7 kV due to insufficient voltage to overcome the surface tension of the suspension, and at 15 kV, we observed the formation of beads instead of fibers (Figure S1, Supporting Information).

Generally, in electrospinning, a pseudoplastic spinning dope with a relatively high apparent viscosity (compared with QD suspensions) is used; most QD suspensions are quite low in viscosity as each QD is relatively independent with weak long-range interactions. In our study here, however, the use of mesophase CdS MSCs suspended in chloroform, result in a viscoelastic solid (Figure S2A, Supporting Information), with a tangent delta,  $\tan(\delta) < 1$ , achieved through its supramolecular mesophase behavior. We fit the shear rate-dependent behavior of the QD

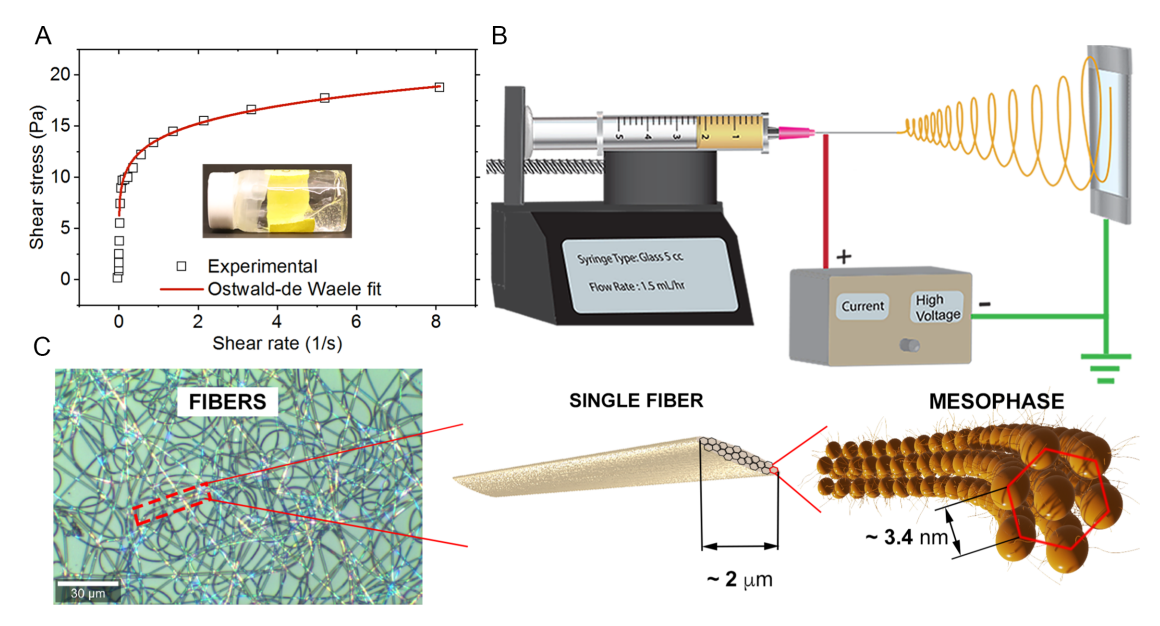


Figure 1. A) Rheology data for CdS MSC electrospinning suspension fit to Ostwald–de Waele power law where  $n=0.153\pm3.59\times10^{-3}$  and  $K=13.7\pm7.84\times10^{-2}$  Pa s"; inset image is taken just as CdS MSC electrospinning suspension in chloroform is set on its side to show viscous behavior. B) Traditional electrospinning apparatus consisting of a pump, a high voltage source, and a grounded collector used for electrospinning MSCs with no carrier polymer. C) (left) Optical microscopy image of CdS MSCs electrospun fibers spun at 15 kV, (middle) single electrospun fiber stabilized by CdS mesophase with approximate ribbon width shown, and (right) the theorized CdS mesophase within the fiber with d-spacing  $\approx$ 3.4 nm as determined previously. [16]

www.aem-journal.com

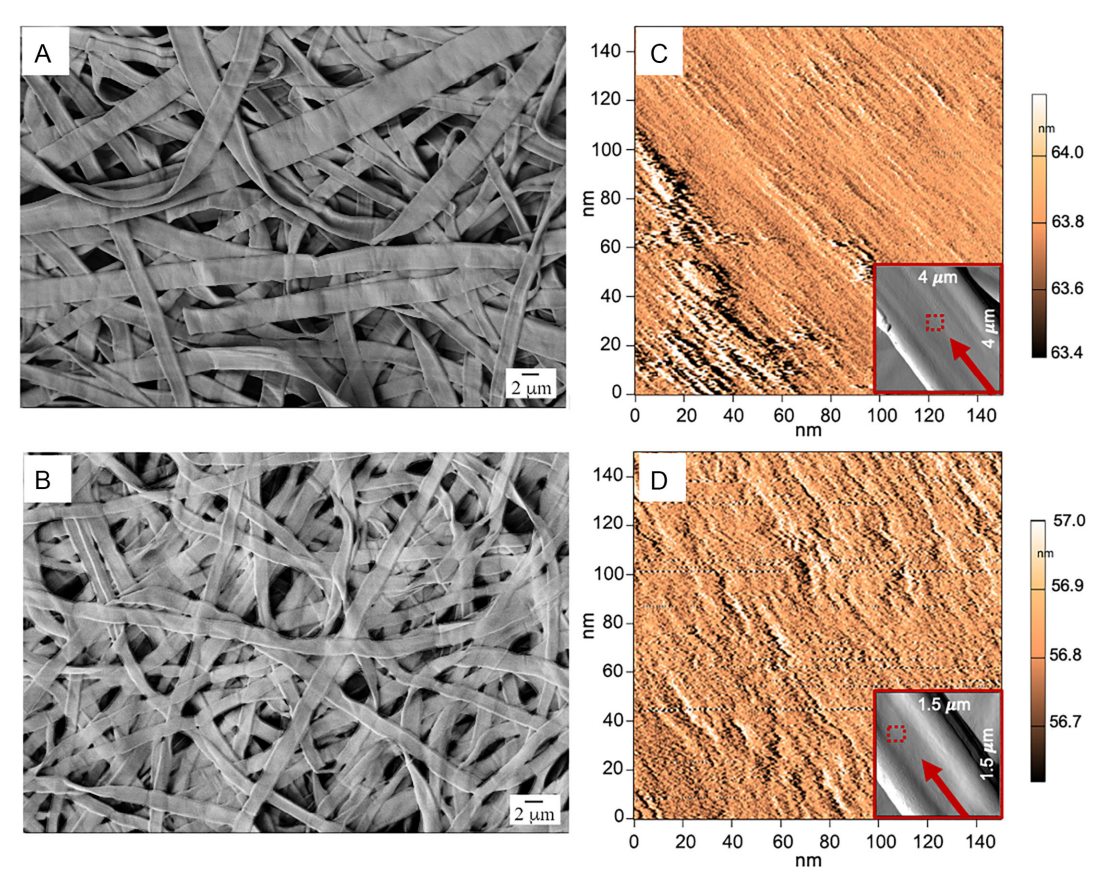


Figure 2. A,B) FE-SEM images from CdS MSCs spun at A) 7 and B) 15 kV having diameters of  $2.5 \pm 0.9$  and  $1.3 \pm 0.4 \,\mu m$ , respectively. C,D) AFM amplitude images of the fiber surfaces of samples spun at C) 7 kV and D) 15 kV with distinct striations going in the direction of the fiber axes. (Insets C and D) Show single-fiber AFM amplitude images with red arrows to represent approximate fiber axis direction. Red squares show approximate locations of where  $150 \times 150 \, \text{micrometer}$  images were taken from. Note: Scales on the side of AFM images are not representative of inset images.

suspension to an Ostwald–de Waele power law given by Equation (1)

$$\sigma = K\dot{\gamma}^n \tag{1}$$

where  $\sigma$  is the shear stress, K is the flow consistency index,  $\gamma$  is the shear rate, and n is the flow behavior index (Figure 1A). We found for the QD electrospinning suspension,  $K=13.7 \, \mathrm{Pa} \, \mathrm{s}^n$  and n=0.153, confirming a non-Newtonian, shear thinning behavior (n<1). This low n value indicates a strong shear thinning behavior. In addition, the zero-shear rate viscosity,  $\mu_0 \approx 250 \, \mathrm{Pa} \, \mathrm{s}$ , is quite high (Figure S2B, Supporting Information). This value is closer to that typically seen in a polymer melt, rather than an electrospinning solution. We therefore also consider the apparent viscosity under the flow conditions of this study. Using the shear rate ( $\gamma$ ) at the nozzle from Equation (2)

$$\dot{\gamma} = \frac{4Q}{\pi r^3} \tag{2}$$

where the flow rate  $Q = 1.5 \,\mathrm{mL}\,\mathrm{h}^{-1}$  and  $r = 0.305 \,\mathrm{mm}$  is the inner radius of the needle, we find the shear rate to be  $\dot{\gamma} \approx 19 \,\mathrm{s}^{-1}$ . Although this value is at a shear rate higher than experimentally measured, it is clear the apparent viscosity would be approaching a value below 1 Pa s (Figure S2B, Supporting Information), more

consistent with electrospinning solutions. To further understand the rheology of the suspension, we look at the dimensionless Deborah number (De). We use the Carreau fluid model (Figure S2B, Supporting Information) to determine the relaxation time ( $\lambda = 22.6$  s) of the MSC suspension and calculate the De = 106 from Equation (3)

$$De = \frac{\lambda v_o}{r_o} \tag{3}$$

where  $v_o$  is the initial velocity dictated by the flow rate, and  $r_o$  is the characteristic length that we take as the initial jet radius (i.e., The inner needle radius). At large Deborah numbers (De >> 1), elastic responses hinder the breakup of the electrospinning jet into droplets. Although the MSC suspensions are composed of small molecule QDs, its rheology, with low n and high De values confirm the MSC suspensions behave as if they are a high molecular weight polymer; in turn, this rheology allow these MSC dopes to be successfully electrospun in the absence of a carrier.

The QDs ([(CdS)CdOA<sub>2</sub>]<sub>x</sub>) are decorated with a high mass percent ( $\approx$ 70 wt%) of OA ligands, a small molecule.<sup>[23]</sup> The surface-bound ligands play a pivotal role in directing in the high level of organization of QDs throughout the fiber as seen by the well-oriented diagonal striations along the fiber axis in atomic

www.aem-journal.com

force microscopy (AFM) images that correspond directly to the MSC components (there are no other additives) (Figure 2C,D). From a larger field of view, using AFM and FE-SEM, we observe a ribbon shape; however, the AFM image more clearly reveals a ridge on either side of the fibers (Figure 2, insets C and D, Figure S3, Supporting Information). This pronounced ridge structure suggests the fibers are collapsing during formation. Koombhongse et al. describes the formation of ribbons with tubes forming at the edges. This shape is caused by the skin from either side of the ribbon coming into contact, and is due to the stiffness and charge repulsion of the skin.<sup>[24]</sup> From the highest point to the lowest, the fibers spun at 7 and 15 kV have a fiber thickness of 466  $\pm$  76.2 and 232  $\pm$  29.5 nm, respectively as determined by analyzing height profiles from AFM (Figure S4 and Table S1, Supporting Information). The surface of the samples spun at 7 kV ( $R_0 = 1.45$  nm; see "Atomic Force Microscopy" section under Experimental Section for more information) are rougher than that of the samples spun at 15 kV  $(R_0 = 0.49 \text{ nm})$ . We suspect the thinner fiber diameters resulting from the higher applied voltage increases the packing density of the CdS MSCs (Figure S5, Supporting Information) thereby reducing the overall roughness of the surface.

Based on the combination of FE-SEM and AFM characterization earlier, we conclude a lower applied voltage results in a wider, thicker, and rougher fiber than those spun at a higher applied voltage; however, more notably, the 7 kV spun fiber has what appears to be a neater and less densely packed structure within the fiber due to reduced stretching from the applied voltage.

After successful fiber formation by electrospinning, CdS MSCs retain their atomic structure and properties. To analyze the atomic structure of CdS MSCs, we carried out X-ray diffraction (XRD) and ultraviolet–visible spectroscopy (UV–vis) (Figure 3). CdS has two atomic forms, wurtzite and zinc blende, which are represented by  $\alpha$  and  $\beta$ , respectively. [25] The X-ray powder diffraction patterns for the CdS MSC fibers were recorded and the unit cell parameters were calculated (Table S2, Supporting Information) from the LaBail profile fit. The zinc blende ( $\beta$ -Cd $_{37}S_{20}$ ) and wurtzite ( $\alpha$ -Cd $_{37}S_{20}$ ) structures were observed for the samples spun at 7 and 15 kV, respectively (Figure 3A,B). Williamson et al. showed isomerization from the  $\alpha$ -Cd $_{37}S_{20}$  of CdS MSCs into the  $\beta$ -Cd $_{37}S_{20}$  form occurring based on water or alcohol absorption, and the reverse isomerization upon desorption. [25] We therefore believe the two structures

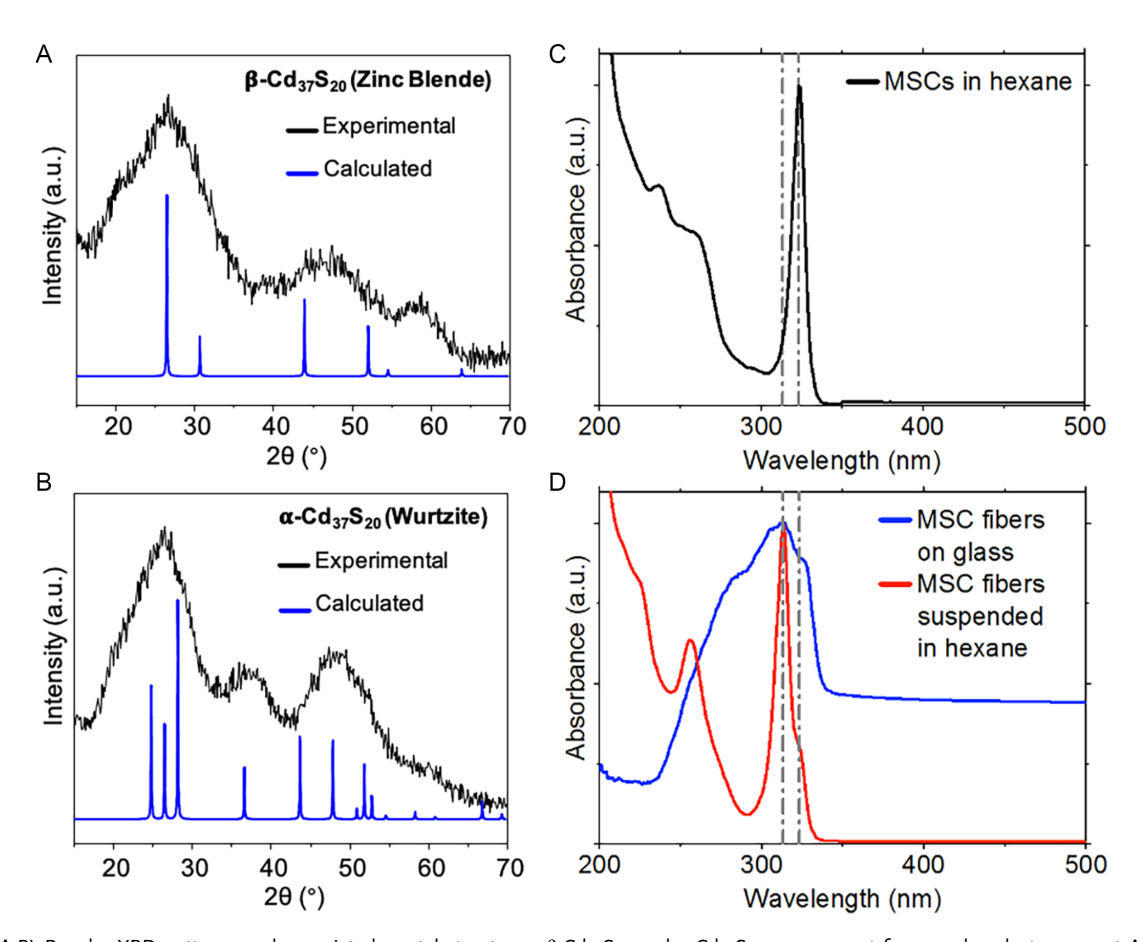


**Figure 3.** A,B) Powder XRD patterns and associated crystal structures, β-Cd<sub>37</sub>S<sub>20</sub> and α-Cd<sub>37</sub>S<sub>20</sub>, are present for samples electrospun at A) 7 kV and B) 15 kV, respectively. C) Absorption spectra for pristine CdS MSCs in hexane, displaying a single excitonic peak at 324 nm, representing the α-Cd<sub>37</sub>S<sub>20</sub> atomic form. D) Absorption spectra of fibers electrospun onto a glass slide at 15 kV, and fibers suspended in hexane after electrospinning display both the α-Cd<sub>37</sub>S<sub>20</sub> and β-Cd<sub>37</sub>S<sub>20</sub> forms, with excitonic peaks located at 324 and 313 nm, respectively.

www.advancedsciencenews.com www.aem-journal.com

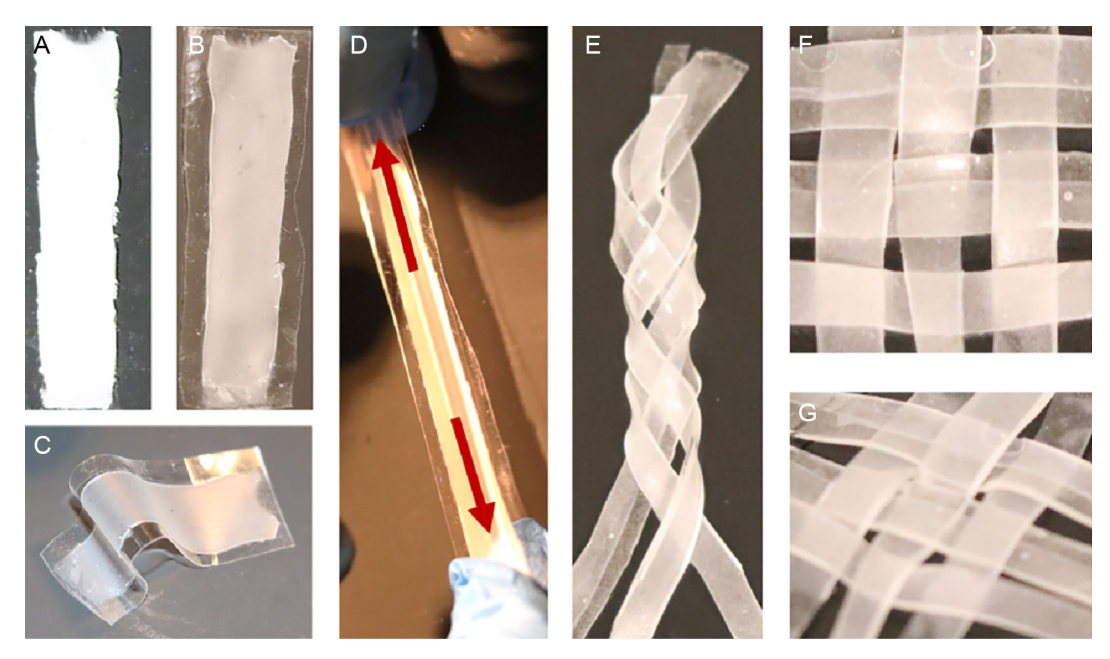


Figure 4. MSC fibers made pliable and modular with elastomer. A) Fibers were first electrospun at 7 kV and deposited on a glass slide. B−D) To increase flexibility, and ease of handling, a fiber/elastomer composite was made by curing an elastomer on top of the fibers deposited on a glass slide, and removing it, thus resulting in a thin layer of fibers coated on one side with elastomer. The fibers/elastomer composite was placed in B) static, C) bending, and D) stretching (≈40% original length) positions. After stretching, the fibers/elastomer composite returned to its original dimensions. E−G) Organization of fibers on the millimeter scale was achieved by fully embedding fibers in elastomer so that they could easily be intertwined and woven into E) a braid and F and G) plain/tabby weave configurations.

observed in XRD for the samples spun at 7 and 15 kV are the result of moisture content and not a result of the electrospinning process. In UV–vis, the two excitonic peaks of CdS MSCs are located at 313 and 324 nm, representing  $\beta\text{-Cd}_{37}S_{20}$  and  $\alpha\text{-Cd}_{37}S_{20}$ , respectively. [25] In our pristine MSCs, without moisture, we observe a peak at 324 nm corresponding to the  $\alpha$  phase (Figure 3C). For the solid fiber sample spun at 15 kV and for redissolved fibers in hexane, without any drying, there is a clear excitonic peak at 313 nm and a hump at 324 nm (Figure 3D). The appearance of 313 nm is indicative of moisture absorption. These findings, along with XRD, confirm the atomic structure of MSCs are preserved throughout the electrospinning process.

By creating and processing CdS MSCs, we are able to create organization over several length scales. From previous research, we know the CdS MSCs organize themselves by molecular selfassembly at the nanometer scale into fibrous structures, please read the study by Nevers et al. for details on this mechanism of ordering. [16] When we electrospin MSCs, we are changing them from a suspension to a compact and organized structure on the nanometer and micrometer scales as observed in AFM and SEM, respectively. Newly formed MSC fibers in this study tend to cling to objects as well as themselves, whereas older fibers become brittle; in both cases, this makes manipulation difficult. To overcome these issues and demonstrate our ability to manipulate and organize fibers on yet another length scale (millimeter), we incorporate an elastomer substrate (Dow SILASTIC MS-4007 moldable silicone) by applying elastomer to fibers spun directly onto a glass slide and peeling the fibers/elastomer off once it was cured (Figure 4A,B). This substrate enables enhanced flexibility. As an example, the fibers/elastomer composite made from fibers spun at 7 kV are able to bend and stretch with limited resistance (Figure 4C.D). When the fibers/elastomer composites are stretched by ≈40% (Figure 4D) and released, the fibers/ elastomer returns to their original dimensions. The mechanical properties of the control elastomer and fully embedded composite (elastomer/fibers/elastomer) are shown in Figure S6, Supporting Information. The maximum machine extension for the samples allows a strain of 1.6, where both control and composite do not break (Figure S6, Supporting Information). With fully embedded fibers, three strands can be cut and intertwined into a braid (Figure 4E). To create the simplest woven structure, we cut these three strands in half, and were able to create a plain/tabby weave design by interlacing the six strands (Figure 4F-G). The hierarchy of these structures span 6+ orders of magnitude starting with the creation of MSCs, then electrospun fibers, and finishing with braids/weaves.

# 3. Conclusions

The formation of the mesophase endows CdS MSCs with high structural stability<sup>[16]</sup> and, more importantly, the CdS MSCs enable electrospinning with no carrier polymer. By electrospinning viscoelastic suspensions of MSCs, we are able to create continuous ribbon fibers of QDs and their ligands with no other additives. We characterized the deposition parameters of these



www.aem-journal.com



fibers and confirmed the crystallographic properties of the MSC are maintained after deposition. The particular electrospinning and weaving of MSCs approach we describe here can organize QD on the nano-, micro-, meso-, and even meter scale, in continuous fibers. The organization of MSCs on the nanometer scale within the electrospun fibers, as we observe in AFM, presents several interesting scientific questions regarding the hierarchical structure of MSCs that will provide rich avenues for future investigation.

For example, the higher applied voltage used during spinning appears to increase the packing density of MSCs due to increased stretching during fiber drawing, thereby lowering the surface roughness. More experimentation into the electrospinning parameters, including a more in-depth analysis and variation of the suspension concentration, flow rate, voltage, and collection method must be carried out to verify this claim. A well-controlled moisture experiment should be conducted to further corroborate that the crystal structures formed are not the result of the electrospinning parameters (i.e., voltage) but rather purely related to the moisture content. In addition, maintaining the order of the MSCs during electrospinning is likely due to 1) the native ordering from the MSC's reported previously, [16] and 2) fiber axis orientation induced by the high strain rate and draw ratio from the applied electric field during electrospinning.<sup>[26]</sup> The validation of this hypothesis, however, will require the creation of new analytical techniques as the transmission electron microscopy (TEM) analysis procedure degrades the particles.<sup>[16]</sup>

Finally, the process that we have outlined for CdS MSCs can potentially be extended to other types of nanostructured building blocks as well as to other fiber drawing methods (e.g., dry spinning and wet spinning). Creating fibers solely of QDs in an economical, simple, one-step process opens up new opportunities for fibrous materials in catalysis, energy harvesting, and chemical sensing.

# 4. Experimental Section

*Materials*: All reagents were used as received, without further purification. Chloroform was purchased from VWR and TCE, and hexane were purchased from Sigma-Aldrich. Materials and methods used to create  $Cd(OA)_2$  and CdS MSCs are described in previous works.<sup>[16,23]</sup>

Electrospinning: CdS MSCs were prepared as previously reported.  $^{[16]}$ Until suspensions were ready to be made, CdS MSCs were stored in a desiccator. We added 3.3 wt% CdS MSCs to chloroform to form with, mechanical agitation, a gel-like suspension. The CdS suspensions underwent mechanical shaking for a minimum of 24 h. When CdS was fully suspended, it was removed from the mechanical shaker, and vortexed. We carried out viscosity measurements on the electrospinning solution (3.3 wt% MSCs) on a TA Instruments AR2000 Rheometer. To examine the effect of varying high voltage, we used 15 and 7 kV (Gamma High Voltage Research Inc.) that were applied to a 1.5 in., 20 gauge disposable needle (Nordson EFD LLC). At both voltages, a flow rate of 1.5 mL h<sup>-1</sup> was applied to our 5 mL glass syringe (Chemglass) using a PH Ultra syringe pump (Harvard Apparatus). Glass slides jacketed in aluminum, were used as grounded collectors. CdS nonwovens were left on the glass slides and when the aluminum jacket was removed, nonwovens were also taken off the jacket for further characterization. A 3.3 wt% Cd(OA)<sub>2</sub> suspension in chloroform was electrospun under the conditions described earlier.

Rheology: To determine the flow properties of the CdS MSC electrospinning suspension, a DHR3 Rheometer was used with a 40 mm  $2^{\circ}$  cone plate. A flow rate sweep was recorded at a constant temperature of

25 °C. The power law fit was carried out using an orthogonal distance regression algorithm. Model parameters, K and n, were acquired form the fit model. The Carreau model was used to fit viscosity data using a Levenberg–Marquardt algorithm. From the fit, we acquired  $\lambda$  and  $\mu_{\rm o}$  of the suspension. Additional rheological parameters,  $\tan(\delta)$ , storage, and loss modulus were determined from an oscillation rate sweep at a constant temperature of 25 °C. All fitting of data was carried out in Origin(Pro), Version (2019) OriginLab Corporation, Northampton, MA, USA.

Field Emission-Scanning Electron Microscopy: We observed the microstructure of CdS fibers using a LEO 1550 FE-SEM. We sputtered samples with gold palladium for 40 s prior to imaging using an SE2 detector at 1 kV accelerating voltage. Using Image J software on several recorded images, we calculated the average fiber ribbon width from at least 50 total measurements gathered from two images. Ribbon widths for samples spun at 15 kV were taken from 150 measurements, from six images, and three different spin dates.

Atomic Force Microscopy: To examine the nano-surface structure of the electrospun fibers, we gathered height and amplitude images in AC mode using an Asylum Research MFP-3D AFM. AFM measurements are carried out on samples electrospun onto glass slides. Roughness measurements were gathered from 150  $\times$  150 nm² images. For samples spun at 7 kV, two measurements were taken, one of the whole image, and one of the upper right hand corner. The second measurement was done due to the protrusions in the lower left of the image that created a higher surface roughness. The  $R_{\rm q}$  of the smaller area from the 7 kV spun sample is 0.77. For samples spun at 15 kV, only the full image roughness measurement is taken.

*Powder XRD*: To determine the crystalline structures of the CdS clusters, after electrospinning, a Bruker D8 Advanced ECO powder diffractometer with a power source of 1 kW Cu K $\alpha$  was used at 40 kV and 25 mA. We removed electrospun samples from the aluminum jackets of glass slides, placed them on the flat backside of a quartz powder holder, and analyzed them between 15 and 70  $2\theta$  for 1162 s. To analyze data, we use GSAS II.<sup>[27]</sup> The calculated and reported<sup>[28,29]</sup> space group parameters for wurtzite and zinc blende are shown in Table S2, Supporting Information.

UV-Vis Spectroscopy: Measurements were carried out on a Cary-5000 spectrometer at a resolution of 0.2 nm. The clusters were measured in a quartz cuvette in hexane. After electrospinning, the fibers were resuspended in hexane for comparison with the pristine MSCs. All spectra had a background subtracted with hexane in a quartz cuvette. For the solid 15 kV electrospun sample, a 3.0 attenuator was used and was in place during background and experimental measurements. A glass slide was baseline subtracted.

Pliable Testbed: We coated the sample spun on a glass slide at 7 kV with a Dow SILASTIC MS-4007 moldable silicone provided by Dow, whereas it was still on the glass slide. The slide was allowed to sit to remove bubbles and then put in an oven to speed up curing process for  $\approx 1$  h. The edges were cut, and the sample was pulled from the glass slide. A thin layer of fibers remained on the glass slide. After stretching and bending, the other side was coated to fully embed the fibers.

## **Supporting Information**

Supporting Information is available from the Wiley Online Library or from the author.

#### **Acknowledgements**

The authors acknowledge the Cornell Center for Materials research staff, Mark Pfeifer and Phil Carubia for instrument training. The auhors also acknowledge Steve Kriske for carrying out AFM measurements and analysis, Phil Carubia for performing Rheometer measurements. The authors thank Emilie Baker and Artemis Xu for advice and training. This work was partially supported by the Cornell Center for Materials Research and



www.aem-journal.com

made use of the Cornell Center for Materials Research Shared Facilities which are funded and supported through the NSF MRSEC program (DMR-1719875).

### Conflict of Interest

The authors declare no conflict of interest.

#### **Author Contributions**

H.H. synthesized  $Cd(OA)_2$  and CdS MSCs, carried out UV-vis measurements, XRD analysis, K.H. synthesized CdS MSCs, L.M.S. carried out electrospinning, rheology analysis, SEM, XRD, UV-vis measurements, and created pliable fiber testbed. All authors contributed to the editing of this article.

# **Data Availability Statement**

The data that support the findings of this study are available from the corresponding author upon reasonable request.

## **Keywords**

cadmium sulfide, electrospinning, mesophase, quantum dots

Received: May 31, 2021 Revised: July 28, 2021 Published online: August 19, 2021

- [1] C. H. Chang, Y. L. Lee, Appl. Phys. Lett. 2007, 91, 053503.
- [2] D. Zhao, C. F. Yang, Renew. Sustain. Energy Rev. 2016, 54, 1048.
- [3] J. Zhai, D. Wang, L. Peng, Y. Lin, X. Li, T. Xie, Sens. Actuators, B Chem. 2010. 147, 234.
- [4] K. Ngamdee, W. Ngeontae, Sens. Actuators, B Chem. 2018, 274, 402.
- [5] Q. Liu, J. Zhu, L. Zhang, Y. Qiu, Renew. Sustain. Energy Rev. 2018, 81, 1825
- [6] S. Wu, J. Li, S. C. Lo, Q. Tai, F. Yan, Org. Electron. 2012, 13, 1569.
- [7] C. L. Zhang, S. H. Yu, Chem. Soc. Rev. 2014, 43, 4423.

- [8] K. Zhang, W. Yuan, N. Zhou, C. Wu, Electrospun Nanofibers for Energy and Environmental Applications, Springer, Berlin Heidelberg, 2014, pp. 403–431.
- [9] R. Liang, D. Yan, R. Tian, X. Yu, W. Shi, C. Li, M. Wei, D. G. Evans, X. Duan, Chem. Mater. 2014, 26, 2595.
- [10] J. S. Jie, W. J. Zhang, Y. Jiang, X. M. Meng, Y. Q. Li, S. T. Lee, Nano Lett. 2006, 6, 1887.
- [11] D. Pisignano, Polymer Nanofibers: Building Blocks for Nanotechnology, Royal Society of Chemistry 2013.
- [12] X. Shi, W. Zhou, D. Ma, Q. Ma, D. Bridges, Y. Ma, A. Hu, I. Nanomater. 2015, 2015, 140716.
- [13] X. Yang, J. Wang, H. Guo, L. Liu, W. Xu, G. Duan, E-Polymers 2020, 20, 682
- [14] M. G. McKee, J. M. Layman, M. P. Cashion, T. E. Long, Science (80-.). 2006, 311, 353.
- [15] M. Allais, D. Mailley, P. Hébraud, D. Ihiawakrim, V. Ball, F. Meyer, A. Hébraud, G. Schlatter, *Nanoscale* 2018, 10, 9164.
- [16] D. R. Nevers, C. B. Williamson, B. H. Savitzky, I. Hadar, U. Banin, L. F. Kourkoutis, T. Hanrath, R. D. Robinson, J. Am. Chem. Soc. 2018, 140, 3652.
- [17] Z. Xu, C. Gao, Acc. Chem. Res. 2014, 47, 1267.
- [18] A. Baji, Y. W. Mai, S. C. Wong, M. Abtahi, P. Chen, Compos. Sci. Technol. 2010, 70, 703.
- [19] M. Mohammadi, P. Alizadeh, F. J. Clemens, *Ceram. Int.* **2015**, *41*, 13417
- [20] S. H. Chen, Y. Chang, K. R. Lee, J. Y. Lai, J. Memb. Sci. 2014, 450, 224.
- [21] S. Agarwal, M. F. Burgard, A. Greiner, W. Joachim, Electrospinning A Practical Guide to Nanofibers, De Gruyter, Berlin 2016.
- [22] J. H. Yu, S. V. Fridrikh, G. C. Rutledge, Polymer (Guildf). 2006, 47, 4789.
- [23] D. R. Nevers, C. B. Williamson, T. Hanrath, R. D. Robinson, *Chem. Commun.* 2017, 53, 2866.
- [24] S. Koombhongse, W. Liu, D. H. Reneker, J. Polym. Sci. Part B Polym. Phys. 2001, 39, 2598.
- [25] C. B. Williamson, D. R. Nevers, A. Nelson, I. Hadar, U. Banin, T. Hanrath, R. D. Robinson, *Science* (80-.). 2019, 363, 731.
- [26] S. Jiang, Y. Chen, G. Duan, C. Mei, A. Greiner, S. Agarwal, *Polym. Chem.* 2018, 9, 2685.
- [27] B. H. Toby, R. B. Von Dreele, J. Appl. Crystallogr. 2013, 46, 544.
- [28] Y. N. Xu, W. Y. Ching, Phys. Rev. B 1993, 48, 4335.
- [29] J. Zemann, Acta Crystallogr. 1965, 18, 139.